

polymer communications

Morphology of reflection holograms formed *in situ* using polymer-dispersed liquid crystals

T. J. Bunning*, L. V. Natarajan, V. P. Tondiglia and R. L. Sutherland

Science Applications International Corporation, 101 Woodman Drive, Suite 103, Dayton, OH 45431, USA

and D. L. Vezie† and W. W. Adams

Materials Directorate, Wright Laboratory, WL/MLPJ, Wright-Patterson AFB, OH 45433-7702, USA

(Received 7 June 1995; revised 29 September 1995)

The morphology of a reflection grating formed using a polymer-dispersed liquid crystalline material system is examined using low-voltage high-resolution scanning electron and transmission electron microscopy. The grating is formed by establishing a fringe pattern in the intensity profile of an argon-ion laser line ($\lambda = 488$ nm) leading to a periodic anisotropic cure through the thickness of the film. The *in situ*, one-step procedure produces periodic layers of polymer- and LC-rich planes lying parallel to the film surface. Droplet diameters are very small (<100 nm) and little coalescence of individual droplets is observed. The grating spacing measured from electron micrographs (153 nm) nearly corresponds to the expected spacing from the observed reflection notch at $\lambda = 472$ nm. Copyright © 1996 Elsevier Science Ltd.

(Keywords: reflection grating; hologram; photopolymerization)

Introduction

Volume holographic materials have been investigated recently for numerous applications in optical data storage, diffractive optics, and various optical interfaces and interconnects. They possess advantages over conventional surface relief gratings in combining high diffraction efficiency with narrow band wavelength and angle selectivity. The formation of both transmission and reflection gratings in photopolymers cured using a fringe pattern (a periodic intensity profile) has been demonstrated^{1,2} to be a viable approach to form volume gratings. The formation of periodic polymer regions separated by voids, generated first by illumination and then by wet chemical processing techniques, generates large periodic refractive index differences through the bulk of a film. Varying the refractive index mismatch by back-filling the voids with low and medium viscosity liquids of known refractive indices has been employed to modulate the performance of these films³.

Extensions of these systems to incorporate liquid crystalline (LC) materials into the pores have also been examined^{4,5}. Because liquid crystals possess a large inherent birefringence and dielectric anisotropy, modulation of the refractive index mismatch between LC-rich areas and polymer-rich areas provides a method of forming electrically switchable holographic elements. These material systems are being developed as programmable beamlet generators, dynamic lenses and optical memory elements^{6,7}.

One such system examined thoroughly is based on

DMP-128, a photopolymer system developed by Polaroid¹. The drawback to this polymer system is the multi-step processing needed to generate the workable optical element. Activation of the photopolymer followed by exposure to a fringe pattern is only the first step. Second, wet chemical etching is needed to generate the pores, and then the LC material must be back-filled into the pores. We have recently demonstrated a one-step, *in situ* method of forming switchable transmission gratings using a different photopolymer system^{8–10}. The LC material is incorporated into the prepolymer syrup before photopolymerization. Upon exposure to a fringe pattern the high-intensity regions photopolymerize (crosslink) fastest, establishing a periodic variation in the rate of curing. The LC molecules diffuse to the low-intensity regions wherein they phase separate into LC-rich lamellae. Switchable transmission Bragg gratings with low switching fields, fast switching speeds, high diffraction efficiency and good optical transparency were formed^{11,12}. We have demonstrated that the one-step process allows for control over the cure kinetics and consequently the final morphology, allowing a variety of performance windows to be accessed. Using these transmission holograms, we also recently demonstrated image storage and electro-optic readout¹³.

We report here for the first time a demonstration of the formation of reflection gratings formed *in situ* using this polymer-dispersed liquid crystal (PDLC) system. These gratings differ significantly from previously reported transmission gratings; specifically in the orientation of the grating planes relative to the surface plane. Although interference is used to prepare both types of structures, major differences in morphology are expected due to changes in the grating spacing which subsequently affects

* To whom correspondence should be addressed

† Current address: The Gillette Company, One Gillette Park 6D-1, South Boston, MA 02127-1096, USA

the balance between photopolymerization kinetics and diffusion. The morphology of these PDLC films is examined using low-voltage, high-resolution scanning electron microscopy (LVHRSEM) and transmission electron microscopy (TEM).

Experimental

The sample components have been discussed previously⁹. The LC content of the prepolymer mixture was 30% and the writing intensity was 50 mW cm⁻². Samples were prepared by placing several drops of the monomer syrup on an indium-tin oxide (ITO) coated glass slide. A second slide was pressed against the first causing the syrup to spread, filling the region between the two ITO plates. Thickness (20 μm) was controlled by uniform spacers. Once assembled, the samples were exposed to an expanded laser beam. A mirror was placed directly behind the sample to obtain the second beam for grating formation. The distance of the mirror from the sample is not critical as long as it is substantially shorter than the coherence length of the laser. Constructive and destructive interference established a periodic intensity profile through the thickness of the film, curing the high-intensity regions the fastest.

Cross-sections of films were prepared by fracturing in liquid N₂, soaking in methanol, and mounting on edge in conductive silver paint. LVHRSEM was conducted on a Hitachi S-900 operating at 1 keV. Very thin conductive coatings (2–3 nm) of tungsten were deposited on the sample surface using a dual-ion beam sputter coater. Samples for TEM were prepared by ultramicrotomy at room temperature from epoxy blocks. Samples were placed in epoxy monomer and cured without further sample preparation. Bright-field TEM was conducted on a Jeol 100CX TEM operating at 100 keV. Section thicknesses were approximately 800 Å. Ultraviolet-visible (u.v.-vis.) spectra were measured on a Perkin-Elmer λ9 UV-Vis-NIR spectrophotometer.

Results and discussion

As discussed in an earlier paper¹⁰, the establishment of an intensity profile through the film leads to an anisotropic, periodic distribution in the rate of photopolymerization. In the reflection geometry employed here, the intensity profile was periodic through the thickness of the film. *Figure 1* shows a series of LVHRSEM micrographs revealing small voids dispersed in the polymer matrix. A fine grating with a periodicity of 156 nm was observed, with the grating vector (indicated by large arrow) perpendicular to the plane of the surface. Thus, individual lamellae of LC-rich and polymer-rich regions run parallel to the surface as indicated by the lines drawn perpendicular to the grating vector. The grating spacing remained constant through the full thickness of the sample from the air/film to film/substrate interface, indicating constant photopolymerization rates as a function of depth.

Unlike transmission holograms formed with similar LC concentrations¹⁰, little coalescence of individual droplets was evident. Very small droplets were present with the majority having diameters between 50 and 100 nm, as shown in *Figure 1c*. Individual droplet diameters as small as 10–20 nm were observed. A slight elongation of some of the droplets was evident with the

major axis parallel to the surface (perpendicular to the grating vector). Smaller arrows on *Figure 1b* clearly indicate that a considerable number of larger droplets have been deformed during the phase-separation process. Unlike transmission gratings, wherein the LC-rich lamellae typically compose <40% of the grating¹⁰, the LC-rich component of the grating for these reflection gratings was much larger. The volume fraction of holes determined using stereology was approximately 20%, indicating that only two-thirds of the LC phase separates out. The fast photopolymerization, as evidenced by the small droplet diameters, undoubtedly traps the remaining third of the LC in the matrix during gelation. The fast polymerization rate also precludes any substantial diffusion of small droplets into larger domains. The different morphology obtained for these reflection gratings when compared with transmission gratings is attributed to the much smaller periodicity for the former case. The time difference between when a high-intensity *versus* a low-intensity region completely cures decreases as the spacing between these two regions becomes smaller. This, in essence, quickens gelation, thereby minimizing droplet growth after phase separation has been initiated. Therefore, small domains with little apparent growth or coalescence are obtained as illustrated by the LVHRSEM micrographs.

The presence of a strong reflection notch in the absorbance spectrum shown in *Figure 2* supports the observation of a periodic refractive index modulation through the thickness of the film. The notch has a reflection wavelength at approximately λ = 472 nm for normal incidence, in addition to a narrow bandwidth. The grating in this sample was written with λ = 488 nm laser radiation. The ~5% difference between the writing wavelength and measured wavelength indicates shrinkage was not a problem for these films. Important in the fabrication of stable gratings, *Figure 2* reveals a notch measured from a sample approximately one year after formation. No decrease in the performance was observed. Leading to this stable performance is the highly functionalized network formed from the penta-acrylate monomer⁹. Upon complete photopolymerization, these films are robust, resisting damage in the electron microscope and change to their physical dimensions with age.

The films meet the Bragg condition for constructive interference dictated by equation (1), which predicts the grating spacing (*d*) of a reflection notch at a known wavelength (λ) and average refractive index (*n*)

$$d = \frac{\lambda}{2n} \quad (1)$$

Using λ = 472 nm and *n* = 1.54 (measured), a predicted spacing of 153 nm is obtained, close to measured value of *d* = 165 ± 16 nm obtained from the LVHRSEM micrographs. Although one would expect higher order reflections due to the non-sinusoidal refractive index distribution, absorption in the u.v. by the polymer host obscures any such reflection notches³.

The TEM micrographs (*Figure 3*) reveal a similar morphology, with distributed regions of polymer-rich material between coarse lamellae of epoxy-filled voids. Epoxy monomer is assumed to displace the LC and, once cured, to occupy the bulk of the voids between the polymer-rich regions. Again, the width of the LC-rich regions was a large fraction of the grating spacing.

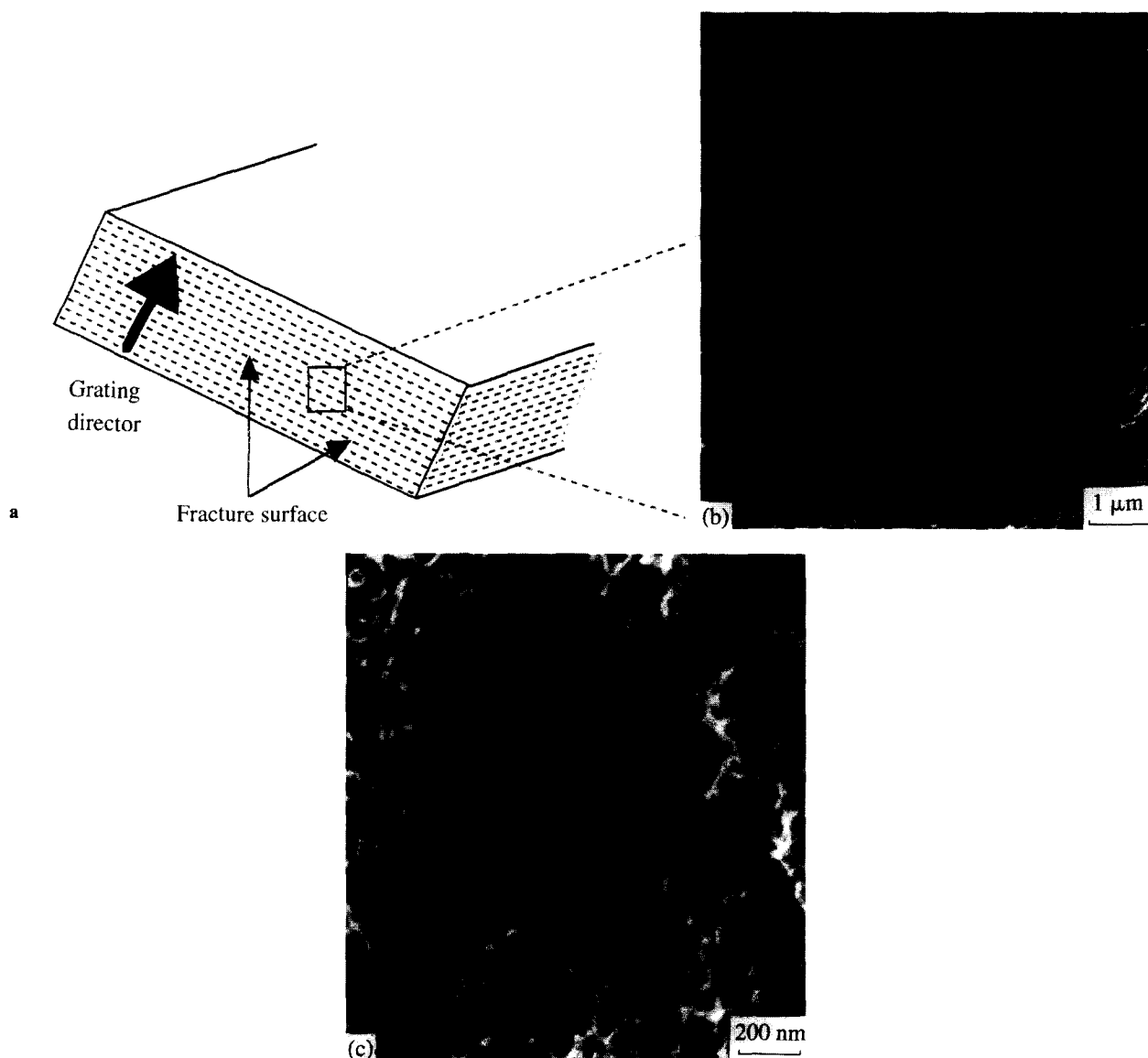


Figure 1 LVHRSEM images of a periodic grating written in a $20\ \mu\text{m}$ thick film using a 488 nm argon-ion laser line in a reflective geometry. The geometry of the film (a) relative to the imaged area at lower magnification (b). The thick black arrow signifies the grating direction while the thinner black arrows show representative droplets of slightly ellipsoidal shape. At higher magnifications (c) droplet sizes and shapes become more apparent although visualization of the grating is lost. Image (b) has the grating planes drawn on the image to aid the eye

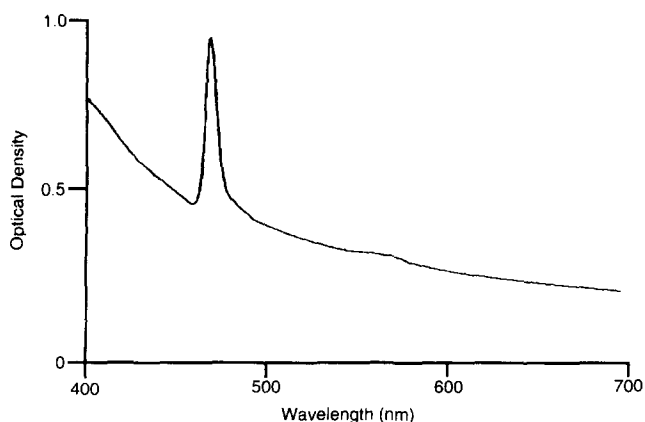


Figure 2 U.v.-vis. spectra taken of the sample imaged in Figure 1 at normal incidence

However, the width of the grating (270 nm) was considerably larger than that measured by SEM. The diameters of the bigger droplets, 150–200 nm, were also considerably larger than observed in the LVHRSEM micrographs. These larger voids were again aspherical with the major axis perpendicular to the surface (parallel to the grating vector). This orientation was opposite to that observed in the SEM and, coupled with the larger grating spacing, may suggest that considerable expansion perpendicular to the grating planes has occurred during sample preparation. Microtomed sections from other reflection grating samples also exhibit this behaviour. The difference in the dimensions of features between LVHRSEM and TEM micrographs is not caused by sample preparation (for viewing). Similar feature sizes on LVHRSEM and TEM micrographs have been observed for transmission gratings prepared under similar conditions¹⁰. Slight discrepancies in the grating spacing would be expected if the cutting plane (and thus

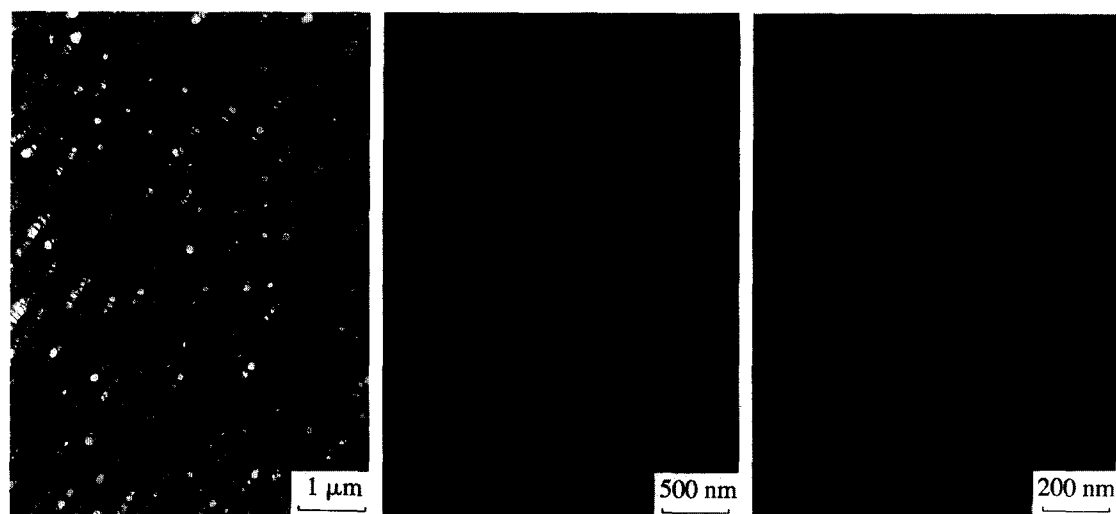


Figure 3 TEM images showing a larger periodicity and domain sizes thought to be due to expansion of the film during sample preparation and subsequent imaging. The black arrow signifies the grating direction

the projection of the grating) was not completely perpendicular to the surface planes. However, the large differences in the droplet diameters observed could not be accounted for using this explanation. Expansion of the larger voids in a direction parallel to the grating vector could account for the ellipticities and spacing observed. Since a large portion of the spacing is accounted for by voids, any substantial change in their size would considerably affect the grating spacing as well. Perhaps the small width of the polymer-rich lamellae leads to substantially weaker lateral (parallel to grating vector) mechanical strength than those cases observed previously wherein the fraction of the polymer-rich lamellae relative to the whole grating spacing (and LC portion) was much larger. The lack of an adequate barrier to expansion could be exaggerated by thin sample thickness. Formation of reflection gratings of larger wavelengths under a variety of cure conditions should be used to examine this discrepancy in more detail. The large difference in spacing and droplet sizes, shapes and ellipticities supports the use of both techniques.

In conclusion, the solid-state morphology of *in situ* generated reflection gratings was explored. The bulk of the droplets are smaller than 100 nm, and little coalescence of individual droplets into larger domains is observed. A grating spacing measured using LVHRSEM corresponds well to that predicted using the measured reflection wavelength. Initial morphological examination using TEM, although showing a periodic distribution of LC and polymer regions, reveals grating spacings and domain sizes considerably larger than observed on

LVHRSEM micrographs. Attempts to modulate the performance of these reflection holograms with an electric field are underway and will be reported at a later date.

Acknowledgements

The first four authors acknowledge support through Air Force Contracts F33600-95-C0055, F33600-93-C0164 and F33615-90-C5911. We also acknowledge the assistance of P. Lloyd in obtaining the TEM images.

References

- 1 Ingwall, R. T. and Fielding, H. L. *Opt. Eng.* 1985, **24**, 808
- 2 Weber, A. M., Smothers, W. K., Trout, T. J. and Mickish, D. J. *SPIE Proc.* 1990, **1212**, 30
- 3 Ingwall, R. T. and Troll, M. *Opt. Eng.* 1989, **28**, 586
- 4 Ingwall, R. T., Troll, M. A. and Whitney, D. H. *US Patent 5 198 912*, 30 March 1993
- 5 Ingwall, R. T. and Adams, T. *SPIE Proc.* 1991, **1555**, 279
- 6 Domash, L., Gozewski, C., Nelson, A. and Schwartz, J. *SPIE Proc.* 1993, **2026**, 642
- 7 Nelson, A. R., Chen, T., Jauniskis, L. and Domash, L. H. *SPIE Proc.* 1995, **2404**, 6
- 8 Sutherland, R. L., Tondiglia, V. P., Natarajan, L. V., Bunning, T. J. and Adams, W. W. *Appl. Phys. Lett.* 1994, **64**, 1074
- 9 Sutherland, R. L., Natarajan, L. V., Tondiglia, V. P. and Bunning, T. J. *Chem. Mater.* 1993, **5**, 1533
- 10 Bunning, T. J., Natarajan, L. V., Tondiglia, V., Sutherland, R. L., Vezie, D. L. and Adams, W. W. *Polymer* 1995, **36**(14), 2699
- 11 Sutherland, R. L., Natarajan, L. V., Tondiglia, V. P., Bunning, T. J. and Adams, W. W. *SPIE Proc.* 1994, **2153**, 303
- 12 Sutherland, R. L., Natarajan, L. V., Tondiglia, V. P., Bunning, T. J. and Adams, W. W. *SPIE Proc.* 1995, **2404**, 132
- 13 Tondiglia, V. P., Natarajan, L. V., Sutherland, R. L., Bunning, T. J. and Adams, W. W. *Opt. Lett.* 1995, **20**, 1325